PERGAMON

Quaternary International 106–107 (2003) 79–88

Pedogenic response to millennial summer monsoon enhancements on the Tibetan Plateau

Xiaomin Fang[a,b,*], Lianqing Lü[b], Joseph A. Mason[c], Shengli Yang[b], Zhisheng An[a], Jijun Li[b], Guo Zhilong[b]

[a] *State Key Laboratory of Loess and Quaternary Geology, Institute of Earth Environment, CAS, Xi'an, Shanxi 710054, China*
[b] *MOE National Laboratory of Western China's Environmental Systems and Department of Geography, Lanzhou University, Lanzhou, Gansu 730000, China*
[c] *Conservation and Survey Division and Department of Geosciences, University of Nebraska, Lincoln, NE, USA*

Abstract

The Asian summer monsoons experienced both rapid, episodic enhancement and long-term evolution with the uplift of Tibet. The response of pedogenesis to those events on the Tibetan Plateau at mean elevations of 4000–5000 m is of great interest and significance in deciphering the history of Asian and Tibetan summer monsoons, and in understanding soil development, deterioration and management. The over 22 m loess–paleosol sequence at Hezuo on the eastern Tibetan Plateau, extending back through the last interglaciation and the thickest late Pleistocene sequence identified thus far on the Plateau, provides a unique opportunity to tackle the above topics. Detailed chronology and soil development determined by field pedofeatures and soil proxies have revealed a millennial fluctuation of the Asian and Tibetan summer monsoons resembling the late Pleistocene North Atlantic climatic record. The end of each Heinrich event is closely followed by formation of a stronger paleosol and then some much weaker thin soil horizons-weathered loess or loess. The episodes of stronger soil development (or paleosol events) correspond without exception to strongest summer monsoon enhancement at the beginning or in the early part of each Bond cycle recorded in the North Atlantic. The strongest pedogenesis and summer monsoon enhancement is observed to occur during 43–36 ka BP, which is not observed in climatic records outside Tibet, probably indicating a coherent enhancement of Asian and Tibetan summer monsoons in the last mega-interstadial (MIS3). Increase of organic matter excluding decomposition and change of soil types from last interglacial calcic cambisols to Holocene chernozems suggests an increase of relative humidity, implying partially an increase of elevation due to late Pleistocene rapid uplift of the Tibetan Plateau.

1. Introduction

During the last glaciation, episodes of extreme cold in polar regions resulted in large discharges of icebergs from continental ice sheets into the North Atlantic Ocean (Heinrich events) (Heinrich, 1988). Each Heinrich event was followed by a sudden return to a climatic regime that was warmer but varied at the millennial scale (D–O events) (Dansgaard et al., 1993; Grootes et al., 1993). The D–O events in turn displayed a long-term temperature decrease toward the next Heinrich event, forming Bond cycles (Bond et al., 1993). These events exerted a strong influence on regions around the north Atlantic (Grimm et al., 1993; Thouveny et al., 1994) and even more distant areas including East Asia (Porter and An, 1995; Ding et al., 1996; Guo et al., 1996; Fang et al., 1999a), the South China Sea (Wang et al., 1999) and the Pacific region (Fukusawa and Koizumi, 1994; Thunell and Mortyn, 1995). The affected Asian monsoons present clear millennial-scale fluctuations resembling climatic change in the North Atlantic region (Porter and An, 1995; Ding et al., 1996; Guo et al., 1996; Fang et al., 1999a; Wang et al., 1999). The extremely cold episodes had serious ecological and environmental effects (e.g., vegetation decimation, desertification, and extremely heavy dust storms), whereas strong summer monsoon enhancement caused rapid return of vegetation cover and a warm-moist climate (An, 2000). The impact of these events on the pedosphere and, in particular, the response of pedogenesis to these events

*Corresponding author. Tel.: +86-29-832-1470; fax: +86-29-832-0456.
E-mail address: fangxm@loess.llqg.ac.cn (X. Fang).

1040-6182/02/$ - see front matter © 2002 Published by Elsevier Science Ltd.
PII: S1040-6182(02)00163-5

is of broad interest in understanding climatic effects on soil development and deterioration, and soil quality evolution and management. Besides these effects, long-term evolution of Asian and Tibetan summer monsoons is closely related to Tibetan uplift. Do these events have an imprint on pedogenesis? Here we provide the highest resolution Pleistocene loess–paleosol sequence obtained thus far from the eastern Tibetan Plateau, to explore the relations between tectonics, climate, and pedogenesis.

2. Geographic setting and paleosol sequence

The Tibetan loess is mostly distributed in large patches on river terraces and basin and planation surfaces in the eastern Tibetan Plateau with mean elevations of ca. 3500–4500 m, with some small patches in its north-central part and in valleys in its southern part (Fang, 1995; Fang et al., 1994, 1999b) (Fig. 1). Its thickness ranges roughly from several to 40 m. Its characteristics are generally similar to that in the Chinese Loess Plateau with elevations of ca. 1200–2000 m (Fig. 1), but its grain size is much coarser than the latter (Fang, 1995). It has been demonstrated that the Tibetan loess comes chiefly from the central and western Tibetan Plateau itself through transport by the high level westerlies and Tibetan winter monsoon (Fang, 1995). The climate in the studied region is largely controlled by the interactions of Asian summer monsoons, Tibetan monsoon and westerlies. Mean

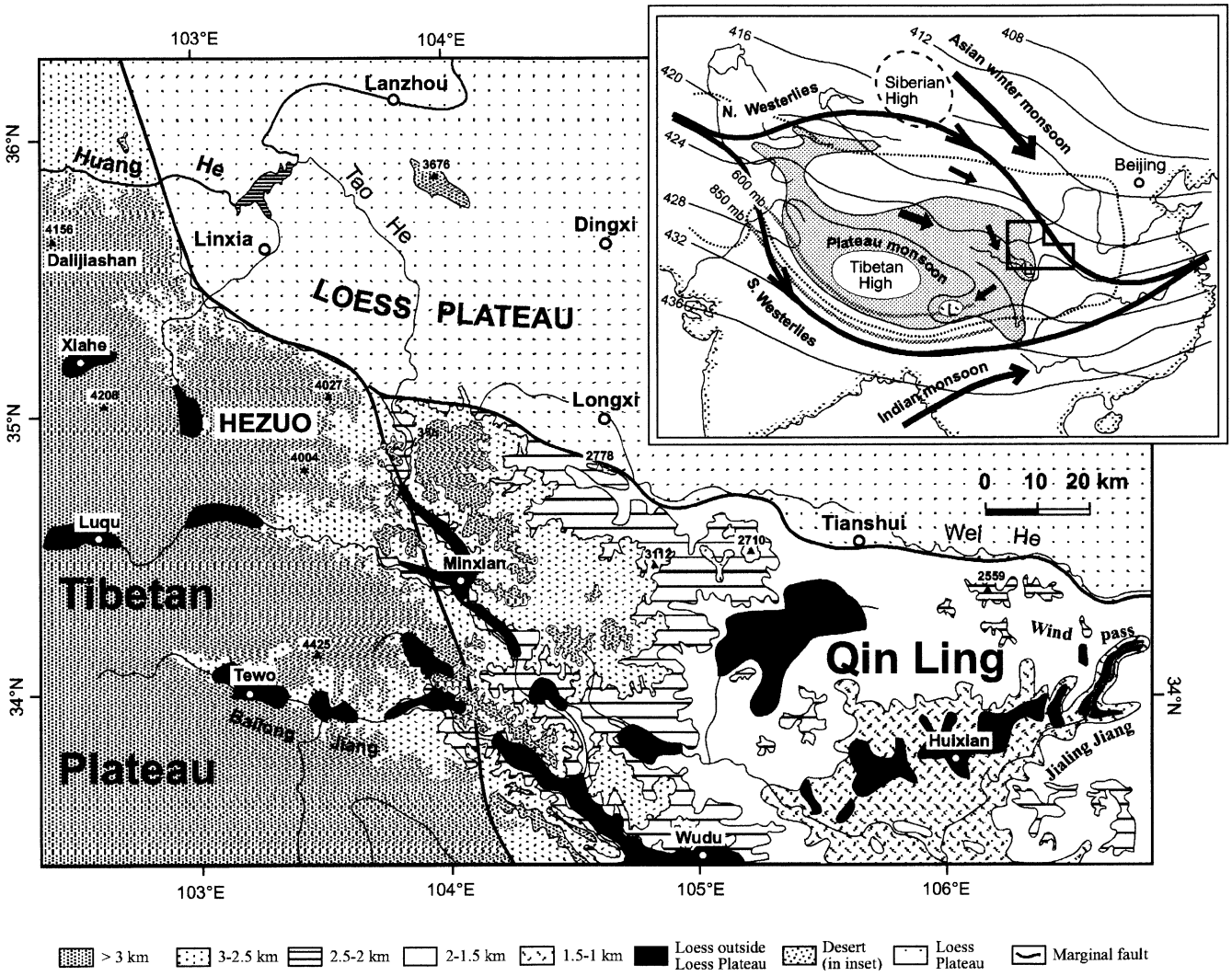

Fig. 1. Location map of the study region, with elevations and loess distribution. The inset shows the configuration of large landforms and wind streamlines indicated by the 700 mbar geopotential height of the January average (Tang et al., 1979). The divergence of the westerlies into north and south branches (jets) at the west end of the Tibetan Plateau and convergence at its east end and in East China in winter, together with mean positions of the Siberian High and Tibetan High, is illustrated. Heavy short arrows indicate average main wind directions responsible for dust transport in and around the Tibetan Plateau in winter and spring. The average January 600 and 850 mbar geopotential heights (light gray continuous lines) indicate the boundary between the Indian and Tibetan monsoons (Tang et al., 1979). Heavy dotted single line marks the area influenced by the Plateau monsoon (Tang et al., 1979). L indicates low pressure centers (cyclones).

Table 1
Climate characteristics of the study area and comparison with neighboring areas

Locality	Elevation (m) Lat–Long.		Month												MAT
			1	2	3	4	5	6	7	8	9	10	11	12	MAP
Hezuo	2915.7	T (°C)	−9.9	−6.7	−1.6	3.5	7.6	10.7	12.8	12.2	8.3	3.2	−3.1	−8.2	2.4
	35.0E–102.9N	P (mm)	3.3	6.0	18.2	30.9	67.1	79.0	110.3	104.7	66.4	37.6	6.3	1.7	531.6
Lanzhou	1517.2	T (°C)	−5.3	−1.0	5.4	12.2	17.0	20.4	22.4	21.2	16.3	9.8	2.5	−3.9	9.8
	36.0E–103.9N	P (mm)	1.4	2.7	9.2	14.7	33.2	44.0	67.0	73.8	40.7	21.3	2.8	0.9	311.7
Linxia	1894.0	T (°C)	−6.7	−3.1	2.7	9.1	13.8	16.0	18.1	17.6	13.2	7.3	1.0	−4.8	7.0
	35.6E–103.2N	P (mm)	3.3	5.4	16.0	31.4	54.9	70.6	101.7	101.4	67.8	35.1	5.7	1.7	494.9
Luochuan	1151.0	T (°C)	−4.4	−1.5	3.9	11.2	16.2	20.2	21.9	20.8	15.7	9.9	3.1	−2.6	9.5
	35.8E–109.5N	P (mm)	5.3	9.7	24.9	36.2	50.5	66.5	130.95	16.6	75.6	47.7	20.5	5.7	590.2
Chaona		T (°C)	−4.6	−2.1	3.1	10.1	14.7	18.8	21.0	19.9	14.9	9.1	2.6	−2.8	8.7
(Lingtai)	35.1E–107.61	P (mm)	6.1	8.8	24.0	44.1	60.5	63.3	116.6	112.1	85.8	54.0	18.7	4.8	599.0

MAT: Mean annual temperature (°C); MAP: Mean annual precipitation (mm).

annual precipitation is 531.6 mm on a 30-year basis (1955–1985). Rain falls mainly from May to September, accounting for 80.4% of mean annual precipitation; winter and spring are very dry (Table 1). Mean annual temperature for the same period is 2.4°C with maximum 12.8°C in July and minimum −9.9°C in January; 5 months have mean temperatures below 0°C (Table 1). Modern soils are mainly chernozems (Xiong and Li, 1990). For comparison, climatic characteristics in Linxia, Lanzhou, Lingtai and Luochuan, where soils locally called Heilu (Zhu et al., 1983; Bronger and Heinkele, 1989; Xiong and Li, 1990) (roughly equivalent to cambisols) occur on surface, are listed as well in Table 1.

The studied section is a fresh landslip surface in Hezuo, Gansu Province, China, in the Hezuo Basin at an elevation of ca. 3000 m, surrounded by the Tibetan main (planation) surface and mountains of ca. 3600–4500 m (Fig. 1). The section is over 22 m thick (the base is unexposed) and is dated back to the penultimate glaciation (see below for details); thus, this is the thickest late Pleistocene loess sequence identified to date on the Tibetan Plateau. It consists of three main parts: the Holocene black soil (S0) at the top, the last glacial yellowish Malan loess (L1) in the middle including eight 30–60 cm thick weak paleosols (Sm0–Sm7) and the last interglacial brownish soil series (S1a–S1b) and Lishi loess at bottom (Fig. 2a). A description of pedofeatures within the section, based on field observations, is as follows:

- Depths 0–1.0 m: Horizon Ah of paleosol S0, very dark grayish brown (10YR 3/2, in dry color by Munsell card (thereinafter)), moderately hard, moderately developed granular ped structure, many biological channels and excrements largely of earth worms, some carbonate coatings in its lower part, gradual lower boundary.
- 1.0–1.5 m: ACk of S0, dull brown (10YR 4/3), hard, blocky-massive, few channels and excrements, many (ca. 30% in area) carbonate thin coatings and $<$ 1 cm impregnations or loose nodules, clear lower boundary.
- 1.5–6.2 m, loess L1L1, light gray (10YR 7/2), loose, massive, few channels land excrements, few carbonate impregnations or small loose nodules; but loess in 4.3–4.8 m presenting some pale brown (10YR 6/3) and carbonate coatings (ca. 15% in area); gradual lower boundary.
- 6.2–6.8 m: Ah of Sm1, light brownish gray (10YR 6/2), moderately hard, massive, some channels and carbonate coatings, gradual lower boundary.
- 6.8–7.7 m: Loess L1L2, pale brown (10YR 6/3), same as loess at depths 1.5–6.2 m, but at its base (7.5–7.7 m) carbonate impregnations and loose nodules reaching ca. 20% in area.
- 7.7–8.8 m: Ah of Sm2, brown (10YR 5/3), moderately hard, massive, channels and carbonate coatings (5% in area), clear lower boundary.
- 8.8–9.5 m: Loess L1L3, pale borwn (10YR 6/3), loose, sandy-coarse silty loam, massive, some channels, some mottles and greenish stains included, gradual lower boundary.
- 9.5–10.1 m: Ah of Sm3a, pale brown (10YR 6/3), moderately hard, blocky-massive, many channels and excrements, some carbonate coatings and nodules, gradual lower boundary.
- 10.1–10.25 m: Ck of Sm3a, light brownish gray (10YR 6/2), hard, many carbonate coatings and nodules, gradual lower boundary.
- 10.25–11 m: Ah of Sm3b, yellowish brown (10YR 5.5/3), same as Sm3a.

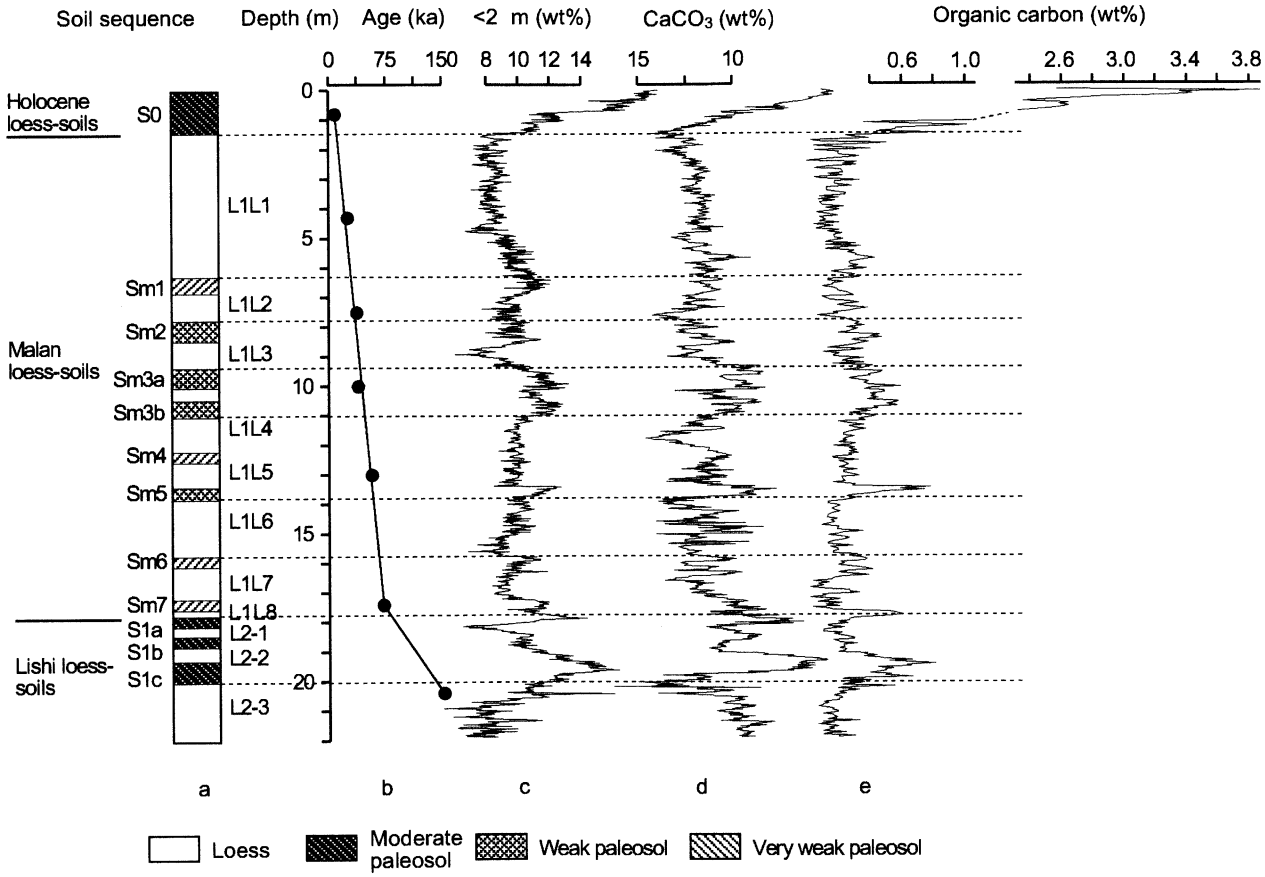

Fig. 2. Loess–paleosol sequence (a) and depth functions of age (b) and contents of clay (c), carbonate (d) and organic matter (e) of the Hezuo loess section.

- 11–11.2 m: Ck of Sm3b, light brownish gray (10YR 6/2), same as Bk of Sm3a.
- 11.2–12.1 m: Loess L1L4, light gray (10YR 7/2), loose, few channels, many carbonate impregnations, some mottles, gradual lower boundary.
- 12.1–12.25 m: Ah of Sm4, yellowish brown (10YR 5.5/3), loose, some channels and excrements, some carbonate coatings, gradual lower boundary.
- 12.25–13.2 m: Loess L1L5, light gray (10YR 7/2), same as loess L1L4.
- 13.2–13.8 m: Ah of Sm5, grayish brown (10YR 5/2.5), moderately hard, many channels and excrements, some small carbonate impregnations or nodules, gradual lower boundary.
- 13.8–14.1 m: Ck of Sm5, light gray (10YR 7/2), hard, few channels, many carbonate coatings, impregnations and fine nodules, gradual lower boundary.
- 14.1–15.8 m: Loess L1L6, pale brown (10YR 6/3), same as loess L1L4.
- 15.8–16 m: Ah of Sm6, brown (10 YR 5/3), same as Sm4.
- 16–17 m: Loess L1L7, very pale brown (10 YR 6.5/3), same as L1L4.
- 17.1–17.3 m: Ah of Sm7, pale brown (10YR 6/3), same as Sm4.
- 17.3–17.5 m: Loess L1L8, light brownish gray (10YR 6.5/2), same as L1L4 but some deeper in color, clear lower boundary.
- 17.5–17.9 m: Bw of S1a, grayish brown (10YR 5/2.5), hard, massive, many channels and excrements, some carbonate coatings, clear lower boundary.
- 17.9–18.1 m: Bk of S1a, light brownish gray (10YR 6.5/2), hard, massive, few channels, 8% in area carbonate coatings and 0.5 cm impregnations or loose nodules, gradual lower boundary.
- 18.1–18.5 m: Loess L2-1, light brownish gray (10YR 6.5/2), moderately hard, some channels and many carbonate impregnations, clear lower boundary.
- 18.5–18.8 m: Bw of S1b, light brownish gray (10YR 6.5/2), same as S1a but with more carbonate coatings and loose nodules at base.
- 18.8–19 m: Loess L2-2, pale brown (10YR 6/3), same as loess L2-1.
- 19–19.8 m: Bw of S1c, dark yellowish brown (10YR 4/4), hard, blocky-massive, ca. 35% in area biological channels and excrements, few carbonate coatings, clear lower boundary.

- 19.8–20.2 m: Bk of S1c, light brownish gray (10YR 6.5/2), hard, massive, few channels, ca. 30% in area carbonate coatings and small nodules, some small mottles, gradual lower boundary.
- 20.2– >22 m: Loess L2-3, pale brown (10YR 6/2.5) with some greenish spots or belts (7.5GY 6/1), moderately loose, massive, some channels and carbonate impregnations, many mottles, base unseen.

3. Sampling and analyses

Bulk samples for soil properties were taken at 2–5 cm intervals along a shallow trench dug on the fresh landslip surface and a total of 910 samples were collected, yielding a resolution of about 100 years per sample. Grain sizes of samples were analyzed on a German Fritsch A22 laser particle sizer, after first removing organic matter and carbonates in boiled H_2O_2 and HCl liquids, respectively, then adding sodium hexametaphosphate and finally dispersing with ultrasound for about 10 min. Carbonate content was analyzed with a standard Bascomb calcimeter (Bascomb, 1961), with two to four analyses per sample yielding an average standard deviation of 0.16 wt%.

4. Chronology

Three organic radiocarbon samples from paleosols and eight thermoluminescence (TL) samples from loesses were taken at different depths to provide age control for the loess–paleosol sequence. The resulting ages are shown in Table 2 and Fig. 2. The ^{14}C ages were first corrected for a half-life of 5568 years and a $\delta^{13}C$ value of 18.3‰ (mean of paleosol S0 on the Loess Plateau; cf. Lin and Li, 1995), then calibrated using a tree ring dataset for ages younger than 18.36 ka (using CALIB3.0, Stuiver and Reimer, 1993) or from a U–Th vs. ^{14}C age dataset for samples older than 18.36 ka (Bard et al., 1990, 1993). The analytical error ranges are smaller than 500 a. An age–depth plot shows two good linear relationships in the Malan loess and paleosol S1 complex, respectively, with a turning point at the boundary of the Malan loess and S1, consistent with reasonable sedimentation rate changes (higher in glacial loess and lower in interglacial soil) (Fig. 2b). Thus, the ages obtained determine the lower boundaries of paleosols S0, Sm2, Sm3, Sm4, and S1 complex and loess L1 at ca. 10 ka, 36 ka, 46 ka, 55 ka, 130 ka, and 75 ka BP, respectively, and the top of paleosol Sm1 at ca. 26 ka BP (Table 2 and Fig. 2). Using this chronology, the loess–paleosol sequence and its corresponding pedogenic and climatic proxy curves strongly resemble the orbital-scale variation in the stacked marine isotopic climatic record (MIS) of the last glacial cycle (Martinson et al., 1987) and in some details the millennial-scale GRIP climatic record of Greenland (Dansgaard et al., 1993) (Fig. 2). Because the TL data have not been calibrated by α and β ray measurements, and their ± 1σ errors ranging from 0.6 to 3.7 ka do not provide sufficient resolution for reconstructing millennial-scale climatic change, we use these dates only as a broad framework of chronology. We refine the chronology by correlating stratigraphic boundaries identified from midpoints of opposed < 2 μm clay peaks with boundaries identified in the marine isotope record (Martinson et al., 1987), assigning the base of S0, base of L1, top of Sm series, and base of Sm series to MIS 1/2 (12.1 ka), MIS 4/5 (73.6 ka), MIS 2/3 (24.1 ka) and MIS 3/4 (59 ka) boundaries, respectively. As well, two additional age controlling points are assigned by correlating the striking peaks (FG8 and FG12) of clay fraction with warm peaks IS8 (34.5 ka) and IS12 (43 ka) of the GRIP ice core record, respectively (Dansgaard et al., 1993). Then, we employ a grain size vs. age model (Porter and An, 1995) based on the assumption that the coarse size fraction is proportional to dust accumulation rate, to calculate ages for all sampling stratigraphic levels between the controlling points. The resulting chronology is consistent with the ^{14}C and TL dates within their error ranges (Table 2 and Fig. 2).

5. Pedogenic response to millennial monsoon changes

Beside qualitative field observations of pedofeatures, quantitative proxies for pedogenesis are used to

Table 2
Chronological constraints for the Hezuo loess section

Depth (m)	Sequence	TL age (ka BP)	^{14}C age (ka BP)	Calendar age (ka BP)	Method or dataset used for calibration
0.8	Lower of S0		7.6±0.28	8.37±0.28	Tree ring chronology (Stuiver and Reimer, 1993)
4.3	Middle of L1L1	25.3±2			
6.8	Bottom of Sm1		21.5±0.51	26.5±0.51	U–Th *vs.* ^{14}C age dataset (Bard et al., 1990, 1993)
7.5	Bottom of L1L2	37±3			
10.0	Bottom of Sm3a		34.8±0.92	39±0.92	U–Th *vs.* ^{14}C age dataset (Bard et al., 1990, 1993)
13.0	Bottom of L1L5	57±4.5			
17.4	Bottom of L1L8	72±6.3			
20.4	Top of L2-3	152±12			

determine degree and type of pedogenesis. The proxies are content of carbonates, organic matter and clay fraction (<2 μm), since they are the most common properties that change during soil formation (FAO-UNESCO, 1988; Xiong and Li, 1990). It is well known that soil formation in Asia is principally controlled by the summer monsoon and most of these pedogenic proxies are also good indicators of summer monsoon change (Fang et al., 1999). Fig. 2 shows the time series of these proxies and their correlations with the climatic records from the GRIP ice core (Dansgaard et al., 1993) and marine sediments (Martinson et al., 1987).

Five main characteristics are immediately apparent. Firstly, the strongest pedogenesis and inferred summer monsoon enhancement as indicated by striking increases in clay fraction and organic matter and decreases in carbonate content occurred in the last interglaciation (MIS5) and Holocene (MIS1), while the weakest pedogenesis and summer monsoon coincides with the earlier (MIS4) and later stadials (MIS2) of the last glaciation. Moderate enhancement of pedogenesis and the summer monsoon occurred in the last mega-interstadial (MIS3) (Fig. 3). This pattern clearly resembles the late Pleistocene marine oxygen isotopic record, reflecting chiefly global ice volume changes (Martinson et al., 1987) (Fig. 3). Secondly, all the major pedogenic and summer monsoon enhancements in the last glaciation appear to coincide approximately with the beginning or early part of Bond cycles in the North Atlantic Ocean (Bond et al., 1993) and match well the large isotopic peaks of the GRIP ice core (Dansgaard et al., 1993), whereas the weakest pedogenesis and summer monsoon occur during the Younger Dryas and Heinrich events (Fig. 3). Thirdly, all the major pedogenic and summer monsoon enhancements in the last glaciation correspond to more strongly developed paleosols identified from field pedofeatures, whereas the strongest pedogenic and summer monsoon enhancements in the last interglaciation and Holocene are correlated with the strongest paleosols S1 and S0, respectively (Fig. 3). Fourthly, distinct pedogenic and summer monsoon enhancements with about half the magnitude

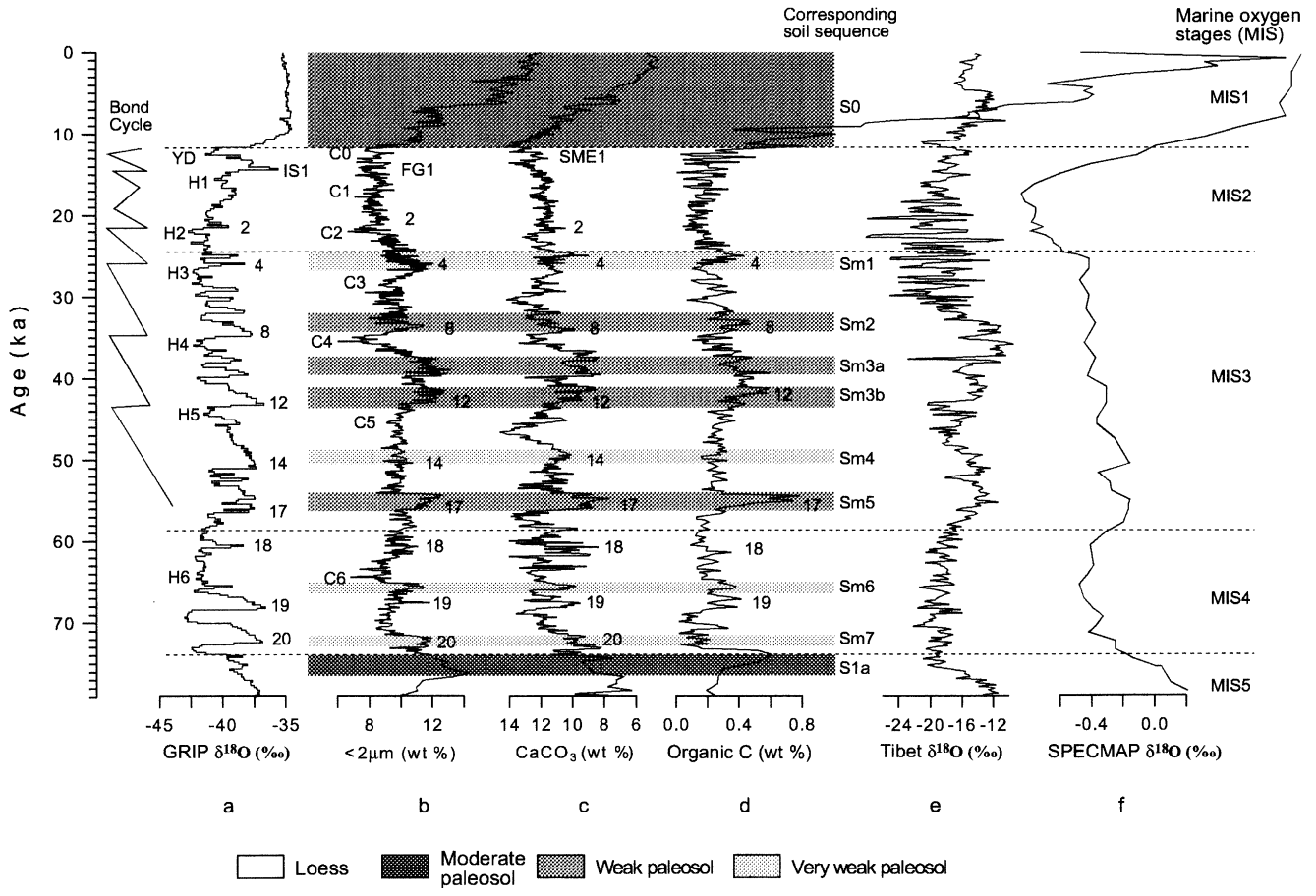

Fig. 3. Variation of pedogenic and summer monsoon proxies (b–d) since the last glaciation and their correlations with the climatic records from the Greenland GRIP ice core (Dansgaard et al., 1993) (a) and SPECMAP of marine sediments (Martinson et al., 1987) (f). Major peaks or troughs of pedogenic and summer monsoon proxies are numbered in relation to the isotopic peaks (IS) of the GRIP ice core, although some weak peaks or troughs cannot easily be assigned numbers. Oxygen isotopic climatic record from the Guliya ice core on the Tibetan Plateau (Thompson and Yao, 1997) (e) and corresponding paleosols (shaded zones) are also plotted for comparison.

observed in the Holocene occurred in ca. 43–36 ka BP (Fig. 3), which is not seen in any climatic records outside of the Tibetan Plateau. Fifthly, there is an obvious long-term trend of increasing organic matter from the last interglaciation to the Holocene (Fig. 3d). Most significant is that soils change accordingly from calcic cambisols to chernozems.

6. Discussion

The orbital- and millennial-scale fluctuations of the pedogenic and summer monsoon proxies, and their similarities to marine and GRIP oxygen isotopic records (Fig. 3) indicate that global ice volume controlled the long-term or background change of the Asian and Tibetan summer monsoons, and the millennial-scale variability of high northern latitude climate has affected the remote and high level monsoons over the Tibetan Plateau, leading to millennial monsoon instability. The Tibetan Plateau is affected by the high latitude westerlies, Asian summer monsoons (mostly Indian monsoon) from lower latitudes or even from the southern hemisphere, and the Tibetan monsoon generated on the Plateau itself (Tang et al., 1979; Tang and Reiter, 1984; Ye and Gao, 1988; Ding, 1991). The Asian winter monsoon seldom extends onto the Tibetan Plateau but flows around its northeastern margin because it is a shallow air system mostly affecting climate under 3000 m a.s.l. (Ding, 1991). The Tibetan monsoon is comprised of summer and winter monsoons because the Plateau has more heat in summer or less heat in winter than its surrounding region. It exerts strong influence on the climate of the Tibetan Plateau and surrounding areas (Tang et al., 1979; Tang and Reiter, 1984; Ye and Gao, 1988). The Tibetan summer monsoon is characterized by distinct low and high pressures at lower and higher levels, respectively, on the Tibetan Plateau, which causes in-flowing winds from the surrounding regions (Tang et al., 1979; Ye and Gao, 1988). The Tibetan Low and High are major factors controlling the onset and intensity of the Indian monsoon at low levels and formation of the exceptionally strong upper level South Asian High (SAH) (Ding, 1991). In most cases, the Tibetan summer monsoon tracks closely with the Indian monsoon (Tang et al., 1979; Ye and Gao, 1988; Ding, 1991), and consequently it is often ignored by Quaternary researchers. To the north of the SAH is the westerly zone located roughly to the north of the Tibetan Plateau in summer and to the south of and on the Plateau in winter. Migration of the SAH or the westerlies will clearly affect the Tibetan climate. Therefore, it is assumed that during Asian and Tibetan summer monsoon enhancements in the last glacial cycle, the SAH was intensified and moved more northwards onto the Tibetan Plateau and caused higher temperature and more precipitation on the Plateau, giving rise to leaching of soil carbonates and fine grains and increasing biological activity, organic matter and soil redness and darkness. When summer monsoon enhancement persists for a certain time interval (ca. 1–2 kyr from our case and soil formation in Lanzhou; cf. Fang et al., 1999a), the ongoing pedogenesis will result in a field-recognizable paleosol (Fig. 3). Unlike climate and soil proxies, a paleosol is an on-earth or lithologic recording of monsoon history and its impacts on soil development, biosphere and ecologic environment. Thus, an episode of summer monsoon enhancement sufficient to produce a field-recognizable paleosol should be called a paleosol event (PE) to highlight its significance. Seven of these paleosol events (PE1–PE7) are observed in the Hezuo section and almost all occurred at the beginning or in the early part of each Bond cycle with sub-orbital periodicity of ca. 6–8 kyr (Fig. 3). During Heinrich events, cold phases would intensify the westerlies, so that they may move completely onto the Tibetan Plateau with a southern branch of the jet kept to the south of the Plateau through the whole year (Fang et al., 1999a). This in turn would enhance flow of polar cold air onto the Plateau, weakening greatly the Tibetan summer monsoon and forcing the Indian monsoon to recede southwards. The combined effect would result in less precipitation and suppress biologic activity and soil development and instead form coarse loess with lightest colors, lowest clay fraction and highest content of carbonates (Fig. 3).

The distinct summer monsoon enhancements ca. 43–36 ka BP is also observed in the oxygen isotopic record of the Guliya ice core on the western Tibetan Plateau, where it was called MIS3 Mega-Warm (Shi et al., 1999) (Fig. 3). The occurrence of this MIS3 Mega-Warm phase seems well established for the Tibetan Plateau, although it has become a topic of debate since it is not recorded outside of the Plateau. Our record shows, however, that the Asian and Tibetan summer monsoon enhancement in response to this Mega-Warm phases only reached a level half that of the Holocene (rather than a higher level than the Holocene in the Guliya ice core; cf. Thompson et al., 1997; Yao et al., 1999) and was weakened greatly in the later part of the MIS3 Mega-Warm (Fig. 3). Shi Yafeng and his co-authors regarded this Mega-Warm phase as a result of considerable enhancement of the Indian monsoon forced by the great contribution of precession during that time interval (Shi et al., 1999). Regardless of the possible mechanism and debate, a stronger paleosol (Sm3) was formed early in the MIS3 Mega-Warm, suggesting that the MIS3 Mega-Warm is at least a local event having considerable environmental impacts.

It is well known that soil organic matter increases generally with elevation due to reduced temperature and increased humidity (Xiong and Li, 1990). Some linear

Table 3
Average organic carbon in paleosols S0 and S1c and their ratios (S0/S1) from the studied section and others on the Chinese Loess Plateau

Location	Elevation (m)	MAT (°C)	Organic C in S0 (wt%)	Organic C in S1c (wt%)	Organic C (S0/S1c)
Hezuo	3000	2.4	2.85 (14)[a]	0.67 (6)[a]	4.25
Yuanbao,[b] Linxia	2145	7	1.24 (10)	0.68 (4)	1.82
Beiyuan, Linxia	2020	7	0.81 (5)	0.47 (6)	1.72
Baitashan, Lanzhou	1620	9.8	0.46 (8)	0.30 (6)	1.53
Chaona, Lingtai	1300	8.7	0.57 (9)	0.43 (7)	1.33
Luochuan	1100	9.5	0.55 (1)	0.39 (1)	1.41
Duanjiapo, Xi'an	804	13.3	0.52 (1)	0.41 (1)	1.27

[a] Data in parentheses indicate numbers of samples averaged.
[b] Data were re-calculated from Wang (1995).

relationships between soil organic matter and elevation have been demonstrated in Russia and North China (Sims and Nielsen, 1986). A gradual slow increase of organic carbon or its ratio $C_{S0/S1c}$ with the increase of elevation is observed for paleosols S0 and S1c from the central to southwestern Loess Plateau (Table 3 and Figs. 1 and 4). Linear regression yields a function,

$$Y(\text{organic } C_{S0/S1c}) = 0.0004\ X(\text{elevation}) + 0.91$$

with the coefficient $R^2 = 0.92$ (Fig. 4)

We know that decomposition of organic matter with time would reduce much of organic matter in paleosols, and that the decomposition is chiefly controlled by climate (temperature and humidity) (FitzPatrick, 1984; Xiong and Li, 1990). If S1c originally had organic carbon content similar to S0, then the ratio of organic $C_{S0/S1c}$ is a measure of decomposition of the organic matter in S1c for the time since the last interglaciation. However, organic $C_{S0/S1c}$ on the Tibetan Plateau is more than twofold of those on the Loess Plateau, obviously deviating from the linear relationship above. Thus, the high value of organic $C_{S0/S1c}$ at the Hezuo section is difficult to explain entirely by decomposition of organic matter in S1c, and can be interpreted as the result of lower temperature and increased humidity on the Tibetan Plateau since the last interglaciation. We argue that the observed long-term trend of increasing organic matter from the last interglaciation to the Holocene (Fig. 3d), together with accordant changes of soil types from calcic cambisols to chernozems, is at least partially indicative of soil response to a strong uplift of the Tibetan Plateau since the late Pleistocene, also evidenced by neotectonism and geomorphologic evolution in the region (Li and Fang, 1999).

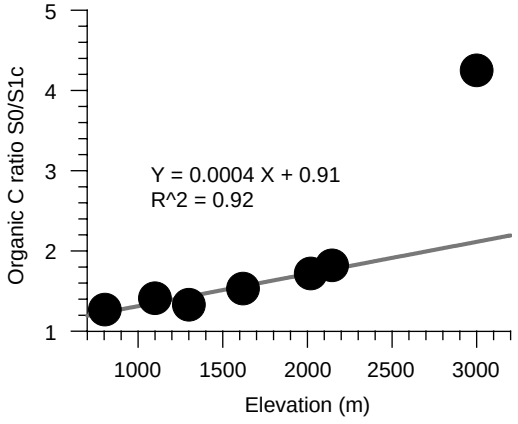

Fig. 4. Variation of the ratio of organic carbon in paleosol S0 and S1c on the Tibetan and Loess Plateaus with elevation.

7. Conclusions

(1) Pedogenesis on the Tibetan Plateau not only has a strong response to orbital-scale variations of glacial–interglacial cycles, but also to large millennial fluctuations of Asian and Tibetan summer monsoons, which are greatly affected by both high and low latitude climates. An enhancement of summer monsoons on the Tibetan Plateau will enhance pedogenesis, whereas persistent intrusion of cold polar air will suppress greatly or even prevent soil formation.
(2) Major enhancements of Asian and Tibetan summer monsoons lasting for ca. 1–2 kyr have caused a complete change of environmental regime, resulting in formation of a paleosol, a physical or lithologic recording of the past eco-environmental system. This is called a paleosol event to highlight its significance.
(3) It is observed that seven obvious paleosol events occurred near the beginning, or in the early part of, each Bond cycle in the North Atlantic Ocean during the last glaciation. The periodicity of occurrence of the paleosol events is roughly 6–8 kyr.
(4) The long-term trend of increasing soil organic matter from the last interglaciation to the Holocene, together with accordant changes of soil types from calcic cambisols to chernozems, may be explained in part by rapid uplift of the Tibetan Plateau since the late Pleistocene.

Acknowledgements

This work was co-supported by the CAS "Hundred Talents Project" (Renjiaozi[2000]005), the Chinese National Key Projects for Basic Research on Tibet Plateau (G1998040809), the NSFC Outstanding Youth Fund (Grant No. 49928101) and MEC Cardreman Teachers Fund. We thank Professors Li Bingyuan and Pan Baotian and Mrs. Yan Maodu, Chen Shiyue, Chen Xiuling, Dong Ming, Xu Xianhai, Miao Yunfa, Long Xiaoyong, and Yang Jiancai for their field or laboratory assistance.

References

An, Z.S., 2000. The history and variability of the East Asian paleomonsoon climate. Quaternary Science Reviews 19, 171–187.

Bard, E., Hamelin, B., Fairbanks, R.G., Zindler, A., 1990. Calibration of the ^{14}C timescale over the past 30,000 years using mass spectrometric U–Th ages from barbados corals. Nature 345, 405–410.

Bard, E., Arnold, M., Fairbanks, R.G., 1993. ^{230}Th and ^{14}C ages obtained by mass spectrometry on corals. Radiocarbon 35 (1), 191–199.

Bascomb, C.L., 1961. A Calcimeter for routine use on soil samples. Chemical Industry 45, 1826–1827.

Bond, G., Broecker, W., Johnsen, S., McManus, J., Labeyrie, L., Jouzel, J., Bonani, G., 1993. Correlations between climate records from North Atlantic sediments and Greenland ice. Nature 365, 143–147.

Bronger, A., Heinkele, Th., 1989. Micromorphology and genesis of paleosols in the Luochuan loess section, China: pedostratigraphic and environmental implications. Geoderma 45, 123–143.

Dansgaard, W., Johnsen, S., Clausen, H.B., Dahl-Jensen, D., Gundestrup, N.S., Hammer, C.U., Hvidberg, C.S., Steffensen, J., Sveinbjörnsdottir, A.E., Jouzel, J., Bond, G., 1993. Evidence for general instability of past climate from a 250 kyr ice-core record. Nature 364, 218–220.

Ding, Y.H., 1991. Advanced Synoptic Meteorology. Meteorological Press, Beijing, p. 792.

Ding, Z.L., Rutter, N.W., Liu, T.S., Ren, J.Z., Sun, J.M., Xiong, S.F., 1996. Correlation of Dansgaard-Oeschger cycles between Greenland ice and Chinese Loess. Paleoclimates 4, 281–291.

Fang, X.M., 1995. The origin and provenance of the Malan loess along the eastern margin of the Qinghai–Xizang (Tibetan) Plateau and its adjacent area. Science in China (B) 38, 876–887.

Fang Xiaomin, Li Jijun, 1999. Review of millennial-scale monsoonal climatic change from paleosol sequences on the Chinese western Loess Plateau and Tibetan Plateau. Chinese Science Bulletin 44 (Suppl. 1), 38–52.

Fang, X.M., Li, J.J., Derbyshire, E., FitzPatrick, E.A., Kemp, R., 1994. Micromorphology of the Beiyuan loess–paleosol sequence in Gansu Province, China: geomorphological and paleoenvironmental significance. Palaeogeography, Palaeoclimatology, Palaeoecology 111, 289–303.

Fang, X.-M., Ono, Y., Fukusawa, H., Pan, B.-T., Li, J.-J., Guan, D.-H., Oi, K., Tsukamoto, S., Torii, T., 1999a. Asian summer monsoon instability during the past 60,000 years: magnetic susceptibility and pedogenic evidence from the Chinese western Loess Plateau. Earth and Planetary Science Letters 168, 219–232.

Fang, X.-M., Li, J.-J., Van der Voo, R., 1999b. Paleomagnetic/rock-magnetic and grain size evidence for intensified Asian atmospheric circulation since 800 kyrs. Earth and Planetary Science Letters 165, 129–144.

FAO-UNESCO, 1988. Soil Map of the World. FAO-UNESCO, Rome, p. 188

FitzPatrick, E.A., 1984. Soils: their Formation, Classification and Distribution. Longman Scientific Technical, Essex, p. 353.

Fukusawa, H., Koizumi, I., 1994. Deep sea sediments in Japan Sea recording the late climatic changes in asia. Chikyu Monthly 16, 678–684 (in Japanese with English abstract).

Grimm, E.C., Jacobson Jr., G.L., Watts, W.A., Hansen, B.C.S., Maasch, K.A., 1993. A 50,000 year record of climate oscillations from Florida and its temporal correlation with the Heinrich events. Science 261, 198–200.

Grootes, P.M., Stuiver, M., White, J.W.C., Johnsen, S., Jouzel, J., 1993. Comparison of oxygen isotope records from the GISP2 and GRIP Greenland ice cores. Nature 366, 552–554.

Guo, Z., Liu, T., Guiot, J., Wu, N., Lu, H., Han, J., Liu, J., Gu, Z., 1996. High frequency pulses of east Asian monsoon climate in the last two glaciations: link with the North Atlantic. Climate Dynamics 12, 701–709.

Heinrich, H., 1988. Origin and consequences of cyclic ice rafting in the Northeast Atlantic Ocean during the past 130 000 years. Quaternary Research 29, 142–152.

Li, J.-J., Fang, X.-M., 1999. Uplift of Qinghai–Tibetan plateau and environmental change. Chinese Science Bulletin 44 (23), 2217–2224.

Lin, B.H., Li, R.M., 1995. Stable isotopic evidence for summer monsoon changes on the chinese loess plateau during the last 800 ka. Chinese Science Bulletin 37 (18), 1691–1693.

Martinson, D., Paisias, N., Hays, J.D., Moore, T.C., Shackleton, N.J., 1987. Age dating and the orbital theory of the ice ages: development of a high-resolution 0-300000 year chronostratigraphy. Quaternary Research 27, 1–30.

Porter, S.C., An, Z.S., 1995. Correlation between climate events in the North Atlantic and China during the last glaciation. Nature 375, 305–308.

Shi Yafeng, Liu Xiaodong, Libingyuan, Yao Tandong, 1999. A very strong summer monsoon event during ka BP in the Qinghai–Xizang Tibet Plateau and its relation to precessional cycles. Chinese Science Bulletin 44(20), 1851–1857.

Sims, Z.R., Nielsen, G.A., 1986. Organic Carbon in Montana soils as related to clay content and climate. Soil Science Society of America Journal 50, 1269–1271.

Stuiver, M., Reimer, P.J., 1993. Extended ^{14}C data base and revised CALIB 3.0 ^{14}C age calibration program. Radiocarbon 35 (1), 215–230.

Tang, M.C., Sheng, Z.B., Chen, Y.Y., 1979. General climatic characteristics of (Tibetan) Plateau Monsoon. Acta Geographica Sinica 34, 33–42.

Tang, M.C., Reiter, E.R., 1984. Plateau monsoons of the northern Hemisphere: a comparison between North America and Tibet. Monthly Weather Review 112, 617–637.

Thompson, L.G., Yao, T.D., Davis, M.E., Henderson, K.A., Thompson, E.M., Lin, P.N., Beer, J., Synal, H.A., Dai, J.C., Bolzan, J.F., 1997. Tropical climate cycle from a Qinghai–Tibetan ice core. Science 276, 1821–1825.

Thouveny, N., de Beaulieu, J., Bonifay, E., Creer, K.M., Gulot, J., Icole, M., Johnsen, S., Jouzel, J., Reille, M., Williams, T., Williamson, D., 1994. Climate variations in Europe over the past 140 kyr deduced from rock magnetism. Nature 371, 503–506.

Thunell, R.C., Mortyn, P.G., 1995. Glacial climate instability in the Northeast Pacific Ocean. Nature 376, 504–506.

Wang, J.M., 1995. Loess and environment change in the northeastern part of Qinghai–Xizang Plateau during the past ka BP. Ph.D. Thesis, Lanzhou University, pp. 76–116.

Wang, L., Sarnthein, M., Erlenkeuser, H., Grimalt, J., Grootes, P., Heilig, S., Ivanova, E., Kienast, M., Pelejero, C., Pflaumann, U., 1999. East Asian monsoon climate during the Late Pleistocene: high-resolution sediment records from the South China sea. Marine Geology 156, 245–284.

Xiong, Y., Li, Q.K., 1990. Soils in China. (Ed.), Science Press, Beijing, pp. 15–131.

Yao, T.D., Liu, X.Q., Wang, N.L., 1999. Last glacial abrupt climatic change on the Tibetan Plateau-Correlation of the Guliya ice core and GRIP ice core. Science in China, Series D 29, 98–106.

Ye, D.Z., Gao, Y.X., 1988. Meteorology of the Tibetan Plateau. Science in China Press, Beijing, China, p. 420.

Zhu, X.M., Li, Y.S., Peng, X.L., Zhang, S.G., 1983. Soils of the loess region in China. Geoderma 29, 237–255.